UTILIZING RAMAN SPECTROSCOPY FOR STRESS IMAGING IN MEMS DEVICES

J. Busbee[1], L. Starman[2], M. Ahmer[3], J. Reber[1], W. Cowan[1], J. Maguire[1]

1. *Materials Directorate, Air Force Research Laboratory, Wright-Patterson AFB, OH 45433*
2. *Dept of Electrical Engineering, Air Force Institute of Technology, Wright-Patterson AFB, OH 45433*
3. *Dept of Mechanical and Materials Engineering, Wright State University, Dayton, OH 45435*

MEMS devices are becoming a pervasive part of today's technology world. Currently, MEMS designers have to take residual stresses into account when designing microdevices. A more ideal state would be for the developer to design to function and to control the residual stresses to fit within designed parameters. For this to occur, methods of mapping residual stresses must be found and used. In this paper, micro-Raman spectroscopy is used to map both residual and induced stress in beam structures on silicon MEMS device.

1. INTRODUCTION

In today's world, microelectromechanical systems (MEMS) are unobtrusively becoming a part of our everyday lives. MEMS are used in many applications, such as air bag triggers in automotive applications to MEMS pressure gauges. However, on the scale on which MEMS devices are built, residual stresses can play a major role in the successful use and reliability of the device. In many devices with free standing structures, residual stress can physically warp the device to a degree that the free standing structure either curls upward or touches the substrate and is no longer useful because of 'stiction' effects. In other device applications such as mirror arrays, the change in dimension due to residual stress gradients can destroy the flatness of the mirror surfaces and ruin the end usefulness of the device. However, if the residual stresses can be mapped, and eventually controlled during the manufacturing processes, the designer will no longer be forced to limit his design to the manufacturing stresses. These stresses will in effect be an additional degree of freedom for the MEMS designer.

Several different methods have been used to characterize strain (and through Hooke's Law, stress) in thin films of silicon. Interferometric measurements of deflection and curvature, as well as four point bending apparatus in conjunction with micro-strain gauges yield averaged strain measurements. X-ray diffraction techniques can measure stress but the technique is cumbersome and lacks a high spatial resolution [1]. Micro-Raman spectroscopy is increasingly being used to measure stress in electronic silicon devices. The technique is non-destructive, relatively quick and accurate enough for most stress measurement uses. Since it is an optical technique, it also shows promise as a minimally invasive *in situ* sensor for use during the manufacture of MEMS devices.

2. EXPERIMENTAL

This paper investigates stresses in MEMS devices utilizing micro-Raman spectroscopy (μRS). Raman spectra were obtained using a Renishaw system 2000 Raman microscope used in backscattering. The laser used was an Ar^+ laser at 514.5 nm. Laser power at the sample was limited to 3.0 mW to minimize sample heating. Scanning was accomplished using a stepping XYZ stage with a 1 μm resolution. The MEMS devices used in the experiment were polysilicon structures fabricated using the Cronos Multi-User MEMS Processes, or MUMPs process. The microdevices were wire bonded to a 144 pin grid array (PGA). The PGA was mounted on a test fixture. Scans of these structures were accomplished by focusing the laser through a microscope objective, resulting in a spatial resolution ~ 1μm. The frequency shifts in the Raman spectra were found by fitting the single Raman peak with a Lorentzian function with an error of ~.1 cm^{-1}.

3. THEORY

The goal of this paper is to show that micro-Raman spectroscopy can be used as an effective measure of local stress *in situ*, *i.e.*, that it can be an effective sensor instead of merely a characterization technique. Other papers have shown that μRS is an effective measure of mechanical stress on silicon (Anastassakis, *et al.* 1970; De Wolf, 1996; Siakavellas, *et al.* 1998). To achieve this goal, the focus is not on the precise value of stress, but rather demonstrating that the stress gradients obtained from the μRS mappings are both reasonable and helpful to the MEMS designer. However, to fully understand the data presented in the paper, it is necessary to briefly develop the relevant theory.

Ganesan *et al.* (1970) was one of the firsts to show the effects of strain of diamond structured crystals. The Raman spectra of silicon has one peak at 520 cm-1, which is comprised of triply degenerate k=0 optical phonon modes. Using the following secular equation (< biblio >) can solve the effect of strain on these optical modes:

$$\begin{vmatrix} p\varepsilon_{11}+q(\varepsilon_{22}+\varepsilon_{33})-\lambda & 2r\varepsilon_{12} & 2r\varepsilon_{13} \\ 2r\varepsilon_{12} & p\varepsilon_{22}+q(\varepsilon_{33}+\varepsilon_{11})-\lambda & 2r\varepsilon_{23} \\ 2r\varepsilon_{13} & 2r\varepsilon_{23} & p_{33}+q(\varepsilon_{11}+\varepsilon_{22})-\lambda \end{vmatrix}$$

$$=0 \quad (1)$$

Where p, q, and r are the optical phonon potentials, and ε_{ij} are the strain tensor components. After solving this equation for the eigenvalues, the following equation relates the solution to the shift in the Raman peak frequencies.

$$\lambda_{i,j=1,2,3} = \omega_s^2 - \omega_u^2 \quad (2)$$

ω_s and ω_u are the stressed and unstressed Raman frequencies for the crystal in question. The strain, ε, and stress, τ, can be related using Hooke's Law

$$\begin{bmatrix} \varepsilon_{11} \\ \varepsilon_{22} \\ \varepsilon_{33} \end{bmatrix} = \begin{bmatrix} S_{11} & S_{12} & S_{12} \\ S_{12} & S_{11} & S_{12} \\ S_{12} & S_{12} & S_{11} \end{bmatrix} \begin{bmatrix} \tau_1 \\ \tau_2 \\ \tau_3 \end{bmatrix} \quad (3)$$

where [S] is the elastic compliance matrix reduced for a cubic crystal structure (Nye, 1957). Assuming uniaxial stress, σ, equation (3) reduces to $\varepsilon_{11}=S_{11}\sigma$, $\varepsilon_{22}=S_{12}\sigma$, $\varepsilon_{33}=S_{12}\sigma$. Solving (1), (2) and substituting for ε using (3), and utilizing that fact that the only phonon mode visible in the backscattering mode from a [100] surface is the third yields:

$$\Delta\omega_3 = \frac{1}{2\omega_s}\left[pS_{12} + q(S_{11}+S_{12})\right]\sigma \quad (4)$$

Using the material parameters found in De Wolf (1996), yields for equation (4)

$$\Delta\omega_3\,(cm^{-1}) = -2\times10^{-9}\sigma\,(Pa). \quad (5)$$

It can be seen from equation (5) that for the case of uniaxial stress (and for the case of biaxial stress, although this is not shown) that the Raman shift is linear with the change in stress. The Raman center frequency of unstressed silicon is 520 cm^{-1}. Compressive stress will shift this value upwards while tensile stress will shift this value downward. Using the above equation and taking into account the experimental accuracy of .1 cm^{-1}, this technique can predict the value of stress to within 20 MPa. Using the values reported in Siakavellas (1998), this number drops lower. However, for this set of experiments the error will be larger due to the imperfect assumption of uniaxial stress and due to the fact that the material parameters above are for single crystal silicon, while the MUMPs devices tested are phosphorus doped polycrystalline silicon. Still, the results displayed in the next section should still give a reasonable approximation of the true stress values present in the device. It should also be noted that bulk Hookean values listed above come into question when the size of the device begins to approach the same spatial size as the grain structure. While these devices are not that small, some error will be introduced here as surface effects begin to dominate the structure.

4. RESULTS AND DISCUSSION

As stated in the previous section, the purpose of this paper is to address changes in stress values during the processing and use of MEMS. To this end, a line scan of the cantilever beam structure shown in Fig. 1 was performed across the longitudinal centerline of the cantilever beam both before and after it was released (sacrificial layer removed) using an acid etch.

Fig. 1. Optical micrograph of cantilever beam on MUMPs device.

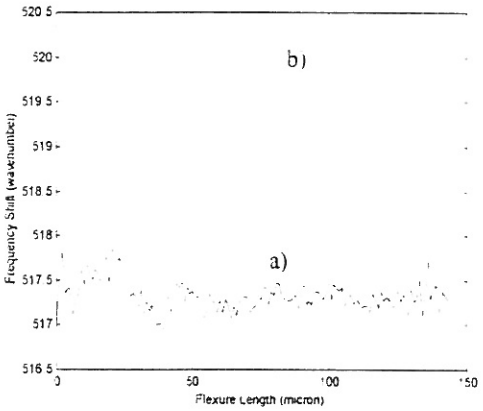

Fig. 2. Raman line scan of a cantilever beam a) before release and b) after release

Fig 2 demonstrates the changes in stress with the release of the structure. In a), before release, the beam has a fairly constant tensile stress profile, while the residual stress in b) is compressive close to the anchor (cantilever) and increases linearly to a tensile state at the end of the structure. The upturn in the data at the end of the graph in b) is the Raman value of the substrate from the scan passing the end of the beam.

The second object to be tested is a micromirror which is a part of a deformable mirror array for use in adaptive optics (Cowan, 1999), as shown in Fig. 3. The mirror is actuated electrostatically using an electrode pad located at the center of the mirror. As

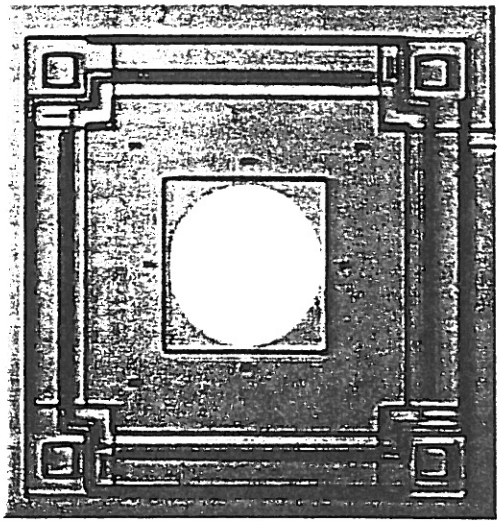

Fig. 3. Optical micrograph is a polysilicon micromirror. The 203 micron mirror is suspended by the surrounding flexures.

part of the MEMS design, dimples located under the flexures prevent 'stiction' effects when snap-down occurs. The flexures surrounding the mirror are constrained from movement by anchors at one end and attached to the mirror at the opposite end. As seen in Fig. 3, the attachment to the mirror is solid. This will allow translation at the end of the flexure, but will resist rotation. The flexure can be modeled as a beam as seen in Fig. 4. As the beam is flexed downward by the actuated mirror, one would expect to see the induced stress distribution on the top of the

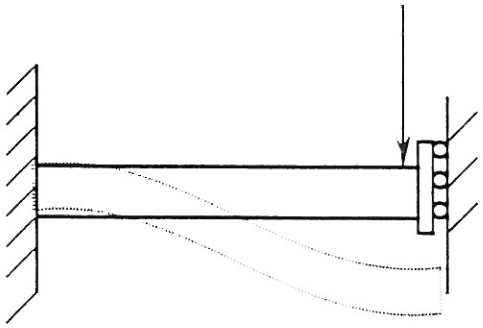

Fig. 4. Beam model of mirror flexure

beam to be essentially s shaped. A tensile stress section should exist close to the cantilever followed by an inflection point and a compressive stress near the right end of the beam. However, Raman measurements of stress include both the induced and residual stresses. To characterize the induced stress first requires the residual stress to be obtained.

Fig. 5 shows both the Raman frequency shift along the longitudinal axis of the flexure well as the resulting residual stress calculated assuming uniaxial stress. The flat region on the left-hand side of both curves corresponds to the physical area of the anchor

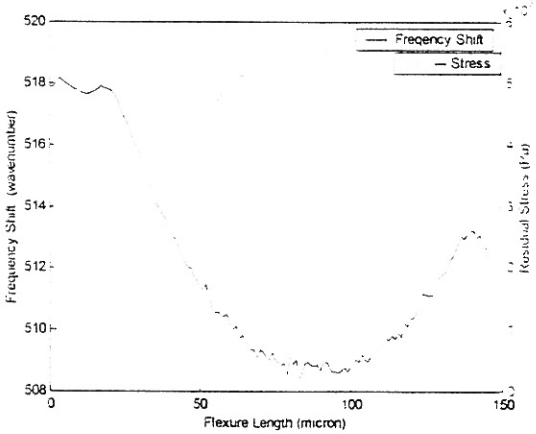

Fig. 5. Stress Distribution along the longitudinal axis of the top flexure. The dotted curve is the residual stress that corresponds to the right hand vertical axis

on the flexure. The stress distribution starts with a small tensile stress close to the anchor and reaches a

maximum of ~6GPa just past the midpoint of the flexure, then begins to relax as it approach the mirror attachment. The assumption of uniaxial stress should be fairly reasonable since the aspect ratio of the mirror is high. However, the geometry of the mirror attachment will add some degree of torsion to the flexure. A rough indicator of the quality of the assumption will be the uniformity of the stress distribution across the short dimension of the flexure. A Raman map was generated of the residual stress in the flexure and is shown in Fig. 6. It is seen in the image, that while there is some variation across the

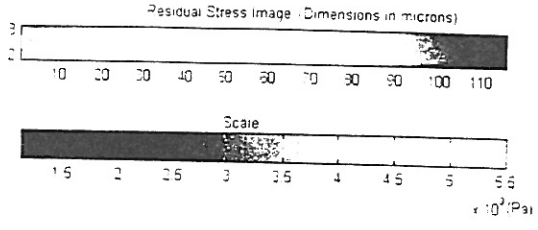

Fig. 6. Raman residual stress image of mirror flexure

short axis, that the color lines, and hence the stress is more or less constant. If the values are examined across the longitudinal axis, the stress distribution obtained in Fig. 5 is reconfirmed. Now that there is a map of the residual stress distribution of the flexure, induced stress across the flexure can be examined. To induce stress in the mirror flexure, the mirror was electrostatically actuated from 0-20 V. To avoid hysteresis effects during the actuation, care was taken to approach the voltage value from the lower side for all measurements. At each voltage setting, a Raman line scan was taken across the same physical dimensions used to find the residual stress distribution in Fig. 5. The residual stress (the stress measured with no electrostatic actuation) was subtracted from each of the corresponding stress distributions to yield the induced stress. The resulting induced stress distributions plotted versus

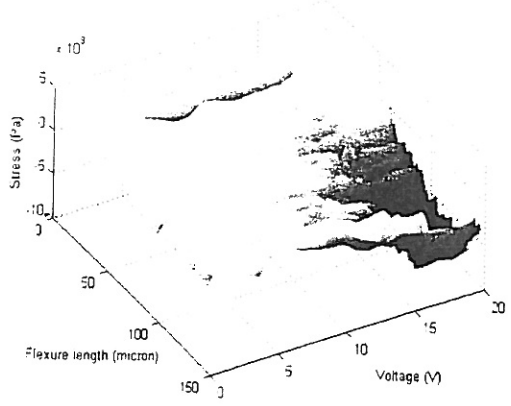

Fig. 7. Stress distributions of a micro-mirror flexure plotted versus increasing electrostatic acuation voltage.

voltage are displayed in Fig. 7. The trough that runs along the rear of the plot once again corresponds to anchor of the flexure. The shape of the curve corresponds well with the nature of electrostatic actuation. The shape changes gradually as voltage is increased. Then, as the snap down voltage is approached, the shape of the curve changes abruptly corresponding to a large change in deflection over a short voltage range. The shape of the induced stress curve in the snap-down region conforms qualitatively to the expected s-shaped distribution for the beam model shown in Fig. 4. That is, there is tensile stress close to the cantilevered left end of the flexure that moves through an inflection point into a compressive stress at the right end of the beam. Another point to be noted from the data on the right-hand side of the graph is the flatness with increasing voltage. Snap-down of the mirror occurs around 16 V. So, between 16 and 20 V there should be no change in stress in the flexure (the flexure is not electrostatically actuated—only the mirror itself is actuated). This flatness helps to confirm the accuracy of micro-Raman spectroscopy in measuring induced stress.

5. CONCLUSIONS

This paper has demonstrated the utility of micro-Raman spectroscopy for measuring both residual and induced stresses in MEMS devices. The stress measurements in the devices were limited to beam shaped devices with high aspect ratios so that the assumption of uniaxial stress was reasonable and so that the resulting shape of the stress distribution could qualitatively confirm that stress values were actually being observed. Future work will include a more rigorous determination of stress via modeling.

REFERENCES

Anastassakis, E. *et al.* (1970). Effect of Static Uniaxial Stress on the Raman Spectrum of Silicon. *Solid State Commun,* Vol. **8** No. 2, 133-138.

Cowan, W. *et al.* (1999). Surface Micromachined Segmented Mirrors for Adaptive Optics. *IEEE J of Sel Topics in Quantum Elect,* Vol. **5**. No. 1, 90-101.

De Wolf. (1996).Micro-Raman spectroscopy to study local mechanical stress in silicon integrated circuits. *Semicond. Sci. Technol.* **11**, 139-154

Nye, J. F. (1957). *Physical Properties of Crystals,* p 140. Oxford Science Publications, Oxford.

Ganesan, *et al.*(1970). *Ann. Phys.* **56**, 556-594.

Siakavellas, M., et al. (1998). Micro-Raman characterization of stress distribution within free standing mono- andpoly-crystalline silicon membranes. *Microelectronic Engineering* **41/42** 469-472